Competition between Antiferromagnetism and Superconductivity in High-T_c Cuprates

David Sénéchal, P.-L. Lavertu, M.-A. Marois, and A.-M. S. Tremblay

Département de Physique and Regroupement Québécois sur les Matériaux de Pointe, Université de Sherbrooke, Sherbrooke, Québec, Canada J1K 2R1

(Received 7 October 2004; published 20 April 2005)

Using variational cluster perturbation theory we study the competition between d-wave superconductivity (dSC) and antiferromagnetism (AF) in the t-t'-t''-U Hubbard model. Large scale computer calculations reproduce the overall ground-state phase diagram of the high-temperature superconductors as well as the one-particle excitation spectra for both hole and electron doping. We identify clear signatures of the Mott gap as well as of AF and of dSC that should be observable in photoemission experiments.

DOI: 10.1103/PhysRevLett.94.156404 PACS numbers: 71.27.+a, 71.10.Fd, 71.10.Pm, 71.15.Pd

Ever since the first paper by Anderson on high-temperature superconductivity [1], most theorists have been working with the premise that the physics of these most intriguing materials should be contained in the two-dimensional one-band Hubbard model. That model of strongly interacting electrons on a two-dimensional square lattice contains a kinetic energy term that represents the band structure, and a potential energy term that accounts only for on-site (perfectly screened) interaction. This simplicity may be too naive, in view of the charge-transfer nature of these compounds. We cannot trust that copper-oxygen planes described by the Hubbard model contain the whole physics until we have shown that the competing phases that are clearly present for both the hole- and electron-doped cuprates, namely, antiferromagnetism (AF) and d-wave superconductivity (dSC), can be reproduced quantitatively by this model. In particular, the model must account for the large range of the AF phase and the small range of the pure dSC phase in electron-doped cuprates, and for the reverse in hole-doped cuprates. Yet recent theoretical studies that found d-wave superconductivity [2,3] concentrated on the hole-doped cuprates. In addition, some authors argue that the one-band Hubbard model description of the cuprates is inadequate to obtain dSC [4] or that additional physical effects must be invoked [5,6].

In this Letter, we show, in agreement with the basic premise of Anderson, that the two-dimensional Hubbard model accounts for the observed doping dependence of the AF and dSC phases as well as for the single-particle excitations for both electron and hole doping. We also identify distinct spectral features of Mott, AF, and dSC physics.

Our results were obtained thanks to new methodology, namely, variational cluster-perturbation theory (VCPT) [7], and because of remarkable increases in computer power made possible by cluster architectures. We study the Hubbard model with interaction U and with hopping parameters that are taken from band structure calculations [8], namely, a diagonal hopping $t' = -0.3t$ and third-neighbor hopping $t'' = 0.2t$.

Variational cluster perturbation theory.—VCPT is an extension of cluster perturbation theory [9] that is based on the self-energy-functional approach [10]. This approach uses the rigorous variational principle $\delta\Omega_{\mathbf{t}}[\Sigma]/\delta\Sigma = 0$ for the thermodynamic grand potential $\Omega_{\mathbf{t}}$ written as a functional of the self-energy Σ:

$$\Omega_{\mathbf{t}}[\Sigma] = F[\Sigma] + \mathrm{Tr}\ln[-(G_0^{-1} - \Sigma)^{-1}]. \qquad (1)$$

The index $\mathbf{t}$ denotes the explicit dependence of $\Omega_{\mathbf{t}}$ on the matrix t_{ij} of hopping terms or, more generally, on *all one-body operators*. That dependence comes through the Green function G_0 of the one-body part of the Hamiltonian. In the above expression, $F[\Sigma]$ is a universal functional of the self-energy obtained from the Legendre transform of the Luttinger-Ward functional. The physical Green function is $G = -\delta F/\delta\Sigma$ [7], and the stationary condition for $\Omega_{\mathbf{t}}[\Sigma]$ gives Dyson's equation. Although F is universal, its exact form is unknown. But all Hamiltonians with the same interacting part share the same functional form of $F[\Sigma]$. Hence $F[\Sigma]$ may be derived from the exact solution of a simpler Hamiltonian H' whose choice of one-body terms makes it exactly solvable. One then looks for stationary solutions within the subspace defined by that simpler solvable problem. The dynamical mean-field theory (DMFT) [11] and cellular-DMFT [12] can be seen as special cases of that approach [7]. The dynamical cluster approximation [13,14] is an alternative self-consistent procedure. In VCPT, one uses for H' a Hamiltonian formed of clusters that are disconnected by removing hopping terms between identical clusters that tile the infinite lattice. H' contains the original Hubbard interaction, hopping, and Weiss fields that are going to be determined by minimizing the grand potential $\Omega_{\mathbf{t}}$. The cluster shape and size can be varied as a check of the relevance of the results to the thermodynamic limit. VCPT is thermodynamically consistent and causal. It goes beyond ordinary mean-field theory, since it predicts the absence of long-range AF order in one dimension [15]. It is also more powerful than variational wave-function approaches [2] since it gives information

about the dynamics of single-particle excitations through the one-particle Green function.

In practice, one proceeds as follows. The universality of F allows us to express the functional $\Omega_{\mathbf{t}}$ in terms of the corresponding functional for the cluster Hamiltonian H', i.e., $\Omega_{\mathbf{t}'}$ in Eq. (5) of Ref. [10]. To include the possibility of broken symmetry one has to allow for this in the variational space for the self-energy that is generated by H'. Hence H' contains the fields M for AF and D for dSC phases:

$$H_M = M\sum_a (-1)^a (n_{a\uparrow} - n_{a\downarrow}), \tag{2}$$

$$H_D = \sum_{a,b} \Delta_{ab} (c_{a\uparrow} c_{b\downarrow} + \text{H.c.}), \tag{3}$$

where $\Delta_{ab} = D$ if sites a and b are nearest neighbors along the x axis and $\Delta_{ab} = -D$ if the sites are nearest neighbors along the y axis. Such a Weiss field cannot be obtained from a Hartree-Fock factorization of the Hubbard model. We stress that no Weiss field or mean-field factorization is allowed in the Hamiltonian H itself. Instead, it is the variational self-energies, $\Sigma = \Sigma(\mathbf{t}')$, that can be accessed that include the variational parameters M and D in the set of variables $\mathbf{t}'$. Rearranging Eq. (5) of Ref. [10] in terms of the cluster grand potential, $\Omega' \equiv \Omega'_{\mathbf{t}}[\Sigma]$ and Green function $G'^{-1} \equiv G_0'^{-1} - \Sigma$, one finds

$$\Omega_{\mathbf{t}}(\mathbf{t}') = \Omega' - \int_C \frac{d\omega}{2\pi} \sum_{\mathbf{K}} \ln\det[1 + (G_0^{-1} - G_0'^{-1})G'], \tag{4}$$

which is the starting point of numerical calculations. The functional trace has now become an integral over the diagonal variables (frequency and superlattice wave vectors) of the logarithm of a determinant over intracluster indices. The frequency integral is carried along the imaginary axis, since it can be shown that the integrand decreases asymptotically as $1/(i\omega)^2$. The minimum of $\Omega(M, D)$ is found using the conjugate-gradient algorithm.

Order parameters.—The treatment of superconductivity in VCPT is best done in the Nambu representation. Translation invariance in the superlattice implies that the Green function $G^{-1} \equiv G_0^{-1} - \Sigma$ depends, after Fourier transformation, on two wave vectors $\mathbf{k}$ and $\mathbf{k}'$ that can differ only by a reciprocal superlattice vector. The electron concentration (n), the AF order parameter (M_o), and the dSC order parameter (D_o) are, respectively, expressed as

$$n = 2i \int \frac{dk}{(2\pi)^2} \int_C \frac{d\omega}{2\pi} \sum_\sigma \mathcal{G}_\sigma(\mathbf{k}, \mathbf{k}, \omega), \tag{5}$$

$$M_o = 2i \int \frac{dk}{(2\pi)^2} \int_C \frac{d\omega}{2\pi} \sum_\sigma (-1)^\sigma \mathcal{G}_\sigma(\mathbf{k}, \mathbf{k} + \mathbf{Q}, \omega), \tag{6}$$

$$D_o = 2i \int \frac{dk}{(2\pi)^2} \int_C \frac{d\omega}{2\pi} \mathcal{F}(\mathbf{k}, \mathbf{k}, \omega) g(\mathbf{k}), \tag{7}$$

where $\mathbf{Q} = (\pi, \pi)$ is the antiferromagnetic wave vector, and $\mathcal{G}_\sigma$ the normal and $\mathcal{F}$ the anomalous VCPT Green functions, written now as functions of wave vector. The dSC form factor is $g(\mathbf{k}) = \cos(k_x) - \cos(k_y)$. The integral over frequencies is carried along the upper half of a clockwise contour that encloses the poles of the Green function up to $\omega = 0$.

Results.—We present VCPT calculations on $L = 6$-site (2×3) and 8-site (2×4) clusters and the 10-site cluster of Ref. [15], using M and D as simultaneous variational parameters and U and μ (the chemical potential) as control parameters. The number of electrons within the cluster (N_c) is a conserved quantity only when the dSC Weiss field D vanishes. When $D \neq 0$, n_c ($n_c = N_c/L$) can take any real value controlled by μ. The calculated electron concentration n [Eq. (5)] is not quantized, even when $D = 0$, except when μ lies within the Mott gap ($n = n_c = 1$). Even though results are displayed as functions of n, one must keep in mind that it is the chemical potential μ that is the true control parameter.

The Weiss fields M and D as a function of μ are obtained from the stationary point (in this case, a minimum) of the grand potential. In VCPT, in sharp contrast with more standard variational approaches, the Weiss fields generally decrease with increasing cluster size since they have to vanish for spontaneous symmetry breaking in an infinite cluster. Instead of the Weiss fields, we show the order parameters as a function of the electron concentration n calculated from Eq. (5), for different system sizes in Fig. 1 and for different interaction strengths in Fig. 2.

The bottom panel showing M_0 in Fig. 1 clearly reproduces the striking contrast between electron-doped ($n > 1$) and hole-doped ($n < 1$) systems. Antiferromagnetism can extend up to about 15% doping on the electron-doped side, while it persists up to only about 6% on the hole-doped side. The dependence on system size is not monotonic because even at fixed cluster size there can be a depen-

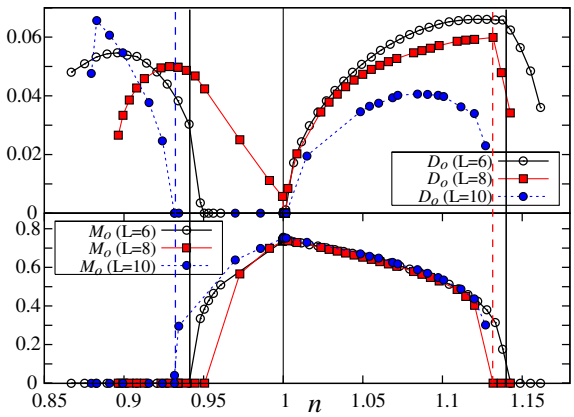

FIG. 1 (color online). AF (bottom) and dSC (top) order parameters for $U = 8t$ as a function of the electron density (n) for 2×3, 2×4, and 10-site clusters. Vertical lines indicate the first doping where only dSC order is nonvanishing.

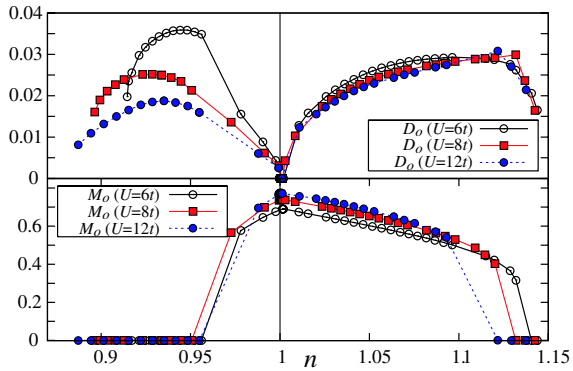

FIG. 2 (color online). AF and dSC order parameters as a function of the electron density on a 2×4 cluster for $U = 6t$, $U = 8t$, and $U = 12t$.

dence on the shape of the cluster. Nevertheless, there is a clear convergence with system size, especially on the electron-doped side. The dSC order parameter is shown in the top panel. For different system sizes, the vertical lines indicate the filling where the dSC phase appears by itself, without AF order parameter. In the electron-doped case, the pure dSC phase is on the right. It survives for a narrow range only, namely, $n = 1.13$ to $n = 1.15$ for $L = 8$, for example. In the hole-doped case, the dSC phase on the left of the vertical lines is present for a range of fillings that is at least twice as large, $n = 0.87$ to $n = 0.93$ for $L = 10$, for example. Unfortunately, finite cluster effects do not allow us to obtain reliable results for larger dopings for either the hole or electron cases. Figure 1 also shows, in the electron-doped case, an AF + dSC phase where AF and dSC order parameters are both nonvanishing [16–18]. We verified that, as expected from symmetry, the π-triplet order parameter is nonvanishing in that phase [19,20], which is separated from a pure dSC phase by a quantum critical point around 13% doping, near the value suggested by experiment [21,22]. The situation is less clear on the hole-doped side where the $L = 6$ cluster has a very small doping range for the AF + dSC phase, the $L = 8$ cluster a large one, while the $L = 10$ cluster shows none. This suggests that the way in which the AF and dSC phases approach each other on the hole-doped side cannot be accurately described by the small variational space that we use. Additional inhomogeneous order parameters, such as stripe [23] or checkerboard orders [24] observed in certain cuprates, may be necessary to get the full picture. No $SO(5)$ symmetric point [25] appears in our calculation in a size-independent way. On the other hand, our results for D_0 in Fig. 1 show unambiguously that the pure dSC phase appears over a much broader range of dopings for hole- than for electron-doped cuprates, as observed experimentally.

It is also instructive to know how the ground-state order parameters vary with interaction strength U, especially because several normal-state calculations for the pseudogap [26,27] show that the interaction strength for electron-doped cuprates near optimal doping should be in the weak to intermediate coupling range ($U \sim 6t$), with U increasing as n decreases. A look at Fig. 2 for D_0 and M_0 shows that the range of dopings where only D_0 is nonvanishing is larger on the hole than on the electron-doped side for all values of U. That range increases with U in all cases so that a drop in U as n increases reinforces the electron-hole difference in the size of the pure dSC region. Note that the magnitude of the dSC order parameter D_0 should not be confused with the critical temperature.

Figure 3 shows intensity plots of the spectral functions at the Fermi level, for $U = 8t$, in the first quadrant of the Brillouin zone. The left illustrates a hole-doped system in a pure dSC phase. The spectral weight is concentrated along the diagonal. This is observed even without long-range order [26], but is also compatible with the vanishing of the dSC gap along the diagonal. On the right, we display an electron-doped system in a AF + dSC phase. The spectral weight is depleted along the diagonal and concentrated near the zone boundaries [$(\pi, 0)$ and $(0, \pi)$]. This is also observed in the absence of long-range order [26], but long-range order makes the plots sharper. The vanishing of the usual dSC gap along the diagonal is offset by the AF gap. The above asymmetric behavior of the spectra on electron- and hole-doped sides is observed in angle resolved photoemission spectroscopy (ARPES) [28,29].

The Mott phenomenon as well as the dSC and AF order parameters each have distinct signatures in the spectral function. The top panel of Fig. 4 illustrates this in the AF + dSC phase for the electron-doped case. The Mott gap, already seen in ARPES [28], corresponds to an absence of states for all wave vectors in the interval $-4t < \omega < -2t$. The two main bands that disperse in the intervals $-8t < \omega < -4t$ and $-t < \omega < 5t$ roughly correspond to those obtained in AF mean-field theory [30]. The AF order parameter manifests itself through the "shadowing" of these main bands by reflection about the magnetic zone boundary. The broad, dispersionless features around $\omega \sim -10t$ and $5t$ are remnants of the atomic limit, intimately related to the Mott phenomenon. The excitations occurring

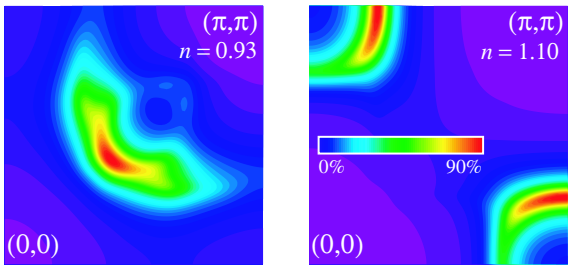

FIG. 3 (color online). Intensity plot of the spectral function at the Fermi level, in the first quadrant of the Brillouin zone, for $U = 8t$ on a $L = 8$ cluster. Left: Hole-doped system ($n = 0.93$). Right: Electron-doped systems ($n = 1.10$). A Lorentzian broadening of $0.2t$ is used.

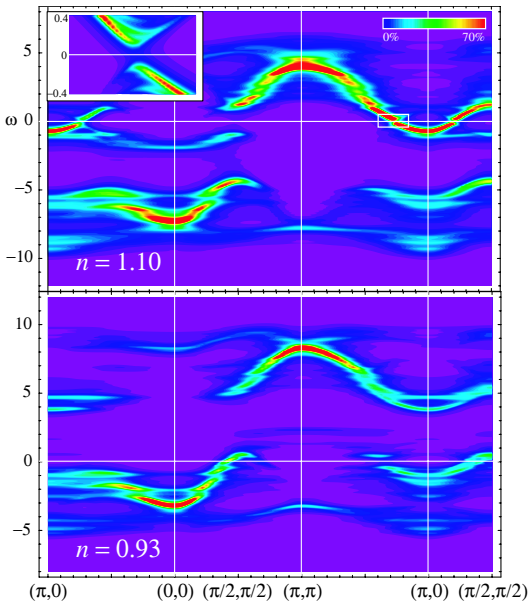

FIG. 4 (color online). Intensity plot of the spectral function as a function of ω in units of t, and wave vector. The Lorentzian broadening is $\eta = 0.12t$ in the main figure and $\eta = 0.04t$ in the inset. Top panel is for the electron-doped case in the right-hand panel of Fig. 3, while bottom panel is for the hole-doped case on the left of Fig. 3.

around $\omega \sim -2t$ are absent at half filling and from the mean-field solution. Their presence, discussed in Ref. [31], considerably reduces the direct gap at $(\pi/2, \pi/2)$. Hints of these new excitations, together with the AF shadowing within the lower-Hubbard band, are seen in ARPES (Fig. 3 of Ref. [28] for $n = 1.04$). The inset, which is a higher-resolution blowup of the rectangular region shown in the figure on the (π, π) to $(\pi, 0)$ segment, shows the dSC gap. The bottom panel of Fig. 4 shows the single-particle spectrum in the hole-doped case. One should be aware, however, that about $2t$ (0.5 eV) below the Fermi energy the spectrum is probably different from that of the hole-doped cuprates because the charge-transfer nature of these compounds manifests itself around that energy, as suggested by recent studies [32] (the corresponding energy falls in the lower-Hubbard band in the electron-doped case). With this proviso, note that additional states also appear in the Mott gap. They are unobservable by ARPES and they are weaker than in the electron-doped case. The broad, dispersionless features remnant of the atomic limit are essentially identical to those of the top panel, except for a rigid shift of about $5t$. More importantly, on the (π, π) to $(\pi, 0)$ segment the pseudogap around $\omega = 0$ is a more dominant feature than the dSC gap. The absence of long-range AF order leads to the absence of shadowing and it makes all excitations much broader near $\omega = 0$, except those at the dSC node near the $(\pi/2, \pi/2)$ point that remain well defined.

Conclusion.—This work shows, within a rigorous variational approach that takes into account short-range dynamics using clusters of different sizes, that the one-band Hubbard model contains the essential physics of the cuprates. It has dSC and AF ground states in doping ranges that are consistent with the observed ones for both electron and hole doping. In addition, low energy excitations manifest in the electronic spectra are shown to be strongly momentum dependent in essentially the same manner as observed using ARPES. Our results also suggest that a quantum critical point on the electron-doped side separates a pure dSC phase from a phase where both AF and dSC order parameters are nonvanishing. In the latter phase, we identified distinct spectral features associated with the Mott gap and with AF and dSC long-range orders that should be observable by ARPES.

We are indebted to V. Hankevych, S. Kancharla, B. Kyung, and M. Norman for useful discussions. This work was supported by NSERC (Canada), FQRNT (Québec), CFI (Canada), CIAR, and the Tier I Canada Research Chair Program (A.-M. S. T.). Computations were performed on a 200-cpu Beowulf cluster and on the 872-cpu Dell cluster of the RQCHP.

[1] P. W. Anderson, Science **235**, 1196 (1987).
[2] A. Paramekanti *et al.*, Phys. Rev. B **70**, 054504 (2004).
[3] T. Maier *et al.*, Phys. Rev. Lett. **85**, 1524 (2000).
[4] S. W. Zhang *et al.*, Phys. Rev. Lett. **78**, 4486 (1997).
[5] F. F. Assaad *et al.*, Phys. Rev. Lett. **77**, 4592 (1996).
[6] G.-H. Gweon *et al.*, Nature (London) **430**, 187 (2004).
[7] M. Potthoff *et al.*, Phys. Rev. Lett. **91**, 206402 (2003).
[8] O. Andersen *et al.*, J. Phys. Chem. Solids **56**, 1573 (1995).
[9] D. Sénéchal *et al.*, Phys. Rev. Lett. **84**, 522 (2000); Phys. Rev. B **66**, 075129 (2002).
[10] M. Potthoff, Eur. Phys. J. B **32**, 429 (2003).
[11] A. Georges *et al.*, Rev. Mod. Phys. **68**, 13 (1996).
[12] G. Kotliar *et al.*, Phys. Rev. Lett. **87**, 186401 (2001).
[13] M. H. Hettler *et al.*, Phys. Rev. B **58**, R7475 (1998).
[14] Th. Maier *et al.*, cond-mat/0404055.
[15] C. Dahnken *et al.*, Phys. Rev. B **70**, 245110 (2004).
[16] M. Inui *et al.*, Phys. Rev. B **37**, 2320 (1988).
[17] E. Demler *et al.*, Phys. Rev. Lett. **87**, 067202 (2001).
[18] A. I. Lichtenstein *et al.*, Phys. Rev. B **62**, R9283 (2000).
[19] G. C. Psaltakis *et al.*, J. Phys. C **16**, 3913 (1983).
[20] B. Kyung, Phys. Rev. B **62**, 9083 (2000).
[21] Y. Dagan *et al.*, Phys. Rev. Lett. **92**, 167001 (2004).
[22] P. Fournier *et al.*, Phys. Rev. Lett. **81**, 4720 (1998).
[23] E. Arrigoni *et al.*, Phys. Rev. B **69**, 214519 (2004).
[24] T. Hanaguri *et al.*, Nature (London) **430**, 1001 (2004).
[25] S. C. Zhang, Science **275**, 1089 (1997).
[26] D. Sénéchal *et al.*, Phys. Rev. Lett. **92**, 126401 (2004).
[27] B. Kyung *et al.*, Phys. Rev. Lett. **93**, 147004 (2004).
[28] N. P. Armitage *et al.*, Phys. Rev. Lett. **88**, 257001 (2002); H. Matsui *et al.*, Phys. Rev. Lett. **94**, 047005 (2005).
[29] F. Ronning *et al.*, Phys. Rev. B **67**, 165101 (2003).
[30] C. Kusko *et al.*, Phys. Rev. B **66**, 140513(R) (2002).
[31] H. Kusunose *et al.*, Phys. Rev. Lett. **91**, 186407 (2003).
[32] A. Macridin *et al.*, cond-mat/0411092.